



# Trabecular bone modeling methodology using geometric representations

*Metodología para el modelado de hueso trabecular empleando representaciones geométricas*

---

Ruiz-Cervantes Osvaldo

Unidad de Investigación y Asistencia Técnica en Materiales (UDIATEM)

Universidad Nacional Autónoma de México

Facultad de Ingeniería

División de Ingeniería Mecánica e Industrial

E-mail: oruiz@unam.mx

Lara-Ramírez José Salvador

Unidad de Investigación y Asistencia Técnica en Materiales (UDIATEM)

Universidad Nacional Autónoma de México

Facultad de Ingeniería

División de Ingeniería Mecánica e Industrial

E-mail: chava\_5694@hotmail.com

Ramírez-Díaz Edgar Isaac

Unidad de Investigación y Asistencia Técnica en Materiales (UDIATEM)

Universidad Nacional Autónoma de México

Facultad de Ingeniería

División de Ingeniería Mecánica e Industrial

E-mail: edgarisaac80@gmail.com

Ortiz-Prado Armando

Unidad de Investigación y Asistencia Técnica en Materiales (UDIATEM)

Universidad Nacional Autónoma de México

Facultad de Ingeniería

División de Ingeniería Mecánica e Industrial

E-mail: armandoo@unam.mx

## Abstract

In this paper is presented a methodology to generate two-dimensional models of cancellous bone from images, with the main objective to achieve a closer representation to reality, in terms of the geometries that can be obtained. The methodology mainly uses Python™ language programming to establish instructions for using Abaqus™ graphical tools and therefore automatically generate the trabecular structure from the original image. As a first step, each trabecula of the image is idealized as an ellipse and each one is taken as basis for generating the geometries of pores and trabeculae in the model. A simulation of a compression test is also presented for three models made with this methodology, where finite element software was used. It is concluded that the methodology allows getting a very similar trabecular structure to the real one.

**Keywords:** cancellous bone, finite element software, trabecular structure, bone modeling.

## Resumen

En este trabajo se presenta una metodología para generar modelos bidimensionales de hueso esponjoso a partir de imágenes, con el objetivo principal de alcanzar una representación más cercana a la realidad en cuanto a las geometrías que se pueden obtener. La metodología usa principalmente el lenguaje de programación Python® para establecer instrucciones de usar las herramientas gráficas de Abaqus® y con esto generar de manera automática la estructura trabecular de la imagen original. Como un primer paso, se idealiza cada trabécula de la imagen como una elipse, y cada elipse se toma como base para generar las geometrías de poros y trabéculas del modelo. También se presenta la realización de un ensayo de compresión para tres modelos hechos con esta metodología, donde se usó paquetería de elementos finitos. Se concluye que la metodología permite obtener una estructura trabecular muy similar a la real.

**Descriptores:** hueso esponjoso, método de elementos finitos, estructura trabecular, modelado de hueso.

## INTRODUCTION

The *Finite Element Method* (FEM) in order to analyze cancellous bone is commonly used for simulations of mechanical tests on models that represent its structure.

A method for creating these models uses data from high resolution microtomography, which directly perform a tridimensional model of the structure through scanning.

However, this method specifically depends on the micro CT resolution. Bevill and Keaveny in 2009 made models, using this method, to be analyzed later by FEM varying the voxel size.

In other cases, it has been preferred to modify the cubic form of the voxels to generate better results, like Depalle who in 2013 changed that shape to a hexahedral and similarly modified the voxel size to get closer results to reality (Depalle *et al.*, 2012).

Other models are based on the trabecular bone representation by a repetition of unit cells to create a com-

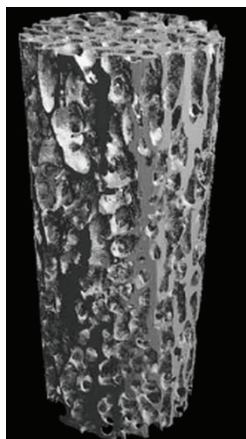


Figure 1. Variation of a trabecular bone model of femoral neck at different voxel sizes: a)  $20\mu\text{m}$  and b)  $120\mu\text{m}$  (Bevill and Keaveny, 2009)

plete structure. Kowalczyk (2003) generated various models using this kind of representation.

In other cases, it was chosen to make two-dimensional models to generate a representation of an image that shows a trabecular bone structure. Ramírez *et al.* (2010) generated two-dimensional models from cancellous bone images obtained by optical microscope, using representations from Voronoi cells.

Other kind of representation idealized each trabecula of a structure using geometric figures. Saha and Wehrli used a methodology based on this in 2004, where they used ellipses to represent each trabecula by scanning points on their periphery, and also a color code was used (Saha and Wehrli, 2004).

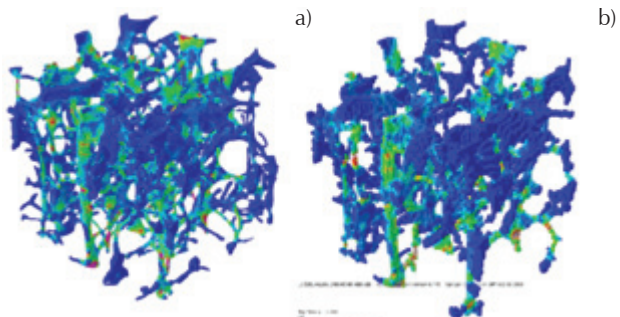
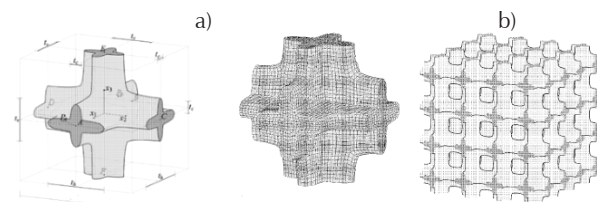


Figure 2. Variation of a vertebral trabecular bone model, with hexahedral voxels of different sizes: a)  $20\mu\text{m}$  and b)  $80\mu\text{m}$  (Depalle *et al.*, 2012)



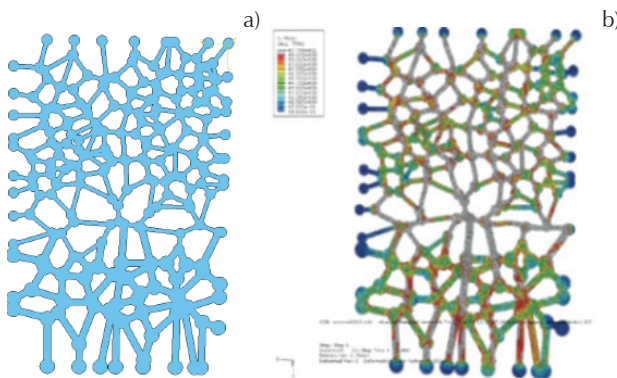


Figure 4. Two-dimensional cancellous bone model through Voronoi cell technique: a) representation and b) representation of equivalent von Mises stress for a compression test (Ramírez et al., 2010)

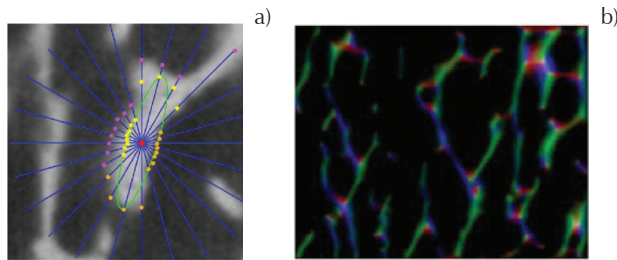


Figure 5. a) Ellipse as representation of a trabecula generated by a scanning method, b) color code for an image of trabecular bone to assign trabeculae dimensions and orientations (Saha and Wehrli, 2004)

## METHODOLOGY

The methodology is based on Saha and Wehrli paper, because a similar representation is used for each trabecula of a structure. The images to develop this methodology were obtained from a bovine femoral specimen, because it is easier to get the samples than from human bone specimen. Subsequently, a portion of the upper epiphysis was selected. That portion was immersed in boiling water, to remove fleshy tissue and red marrow, this process took about 3 hours, under constant water changes. The next step was to immerse the specimen in a hydrogen peroxide solution to 3.5%, in order to detach the remaining residues after boiling. This process took about 16 hours. Once the previous steps were done, it was possible to observe in a better way the trabecular structure, which permitted to identify three significantly different regions:

- Region 1: the trabeculae do not have a preferential orientation. It was seen from greater trochanter to the area named as Ward's triangle.

- Region 2: the trabeculae are oriented diagonally to the direction of the femoral head. This region was seen in the femoral neck and in a previous area to the femoral head.
- Region 3: the trabeculae do not present preferential orientation, however their thickness is visibly greater than the trabeculae in the previous regions. It was seen in the area of the femoral head.

Rectangular areas (2 cm long, 1 cm wide) were selected on the trabecular surface of the specimen (Figure 6).

The reason for selecting areas of that size is to represent the area of the intermediate parallel plane to the main axis of a cylindrical trabecular bone specimen for a compression test. The Figure 7 shows the images of three regions marked by ink.

Then, first coordinates were taken assigning middle points in each trabecula of the cancellous bone, being complex geometries the assigning was performed by the operator. Figure 8 shows an example of midpoints assigned to each trabecula.

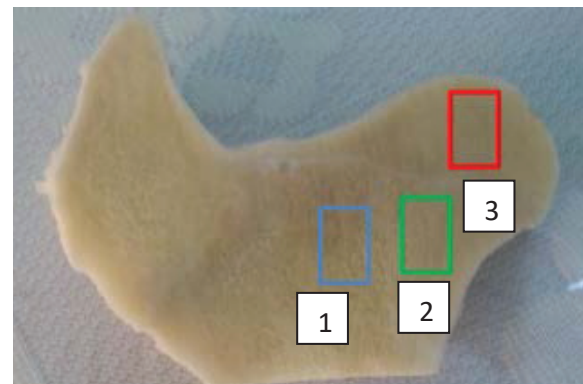


Figure 6. Femur section after removing remaining tissues and analysis areas: region 1, region 2 and region 3

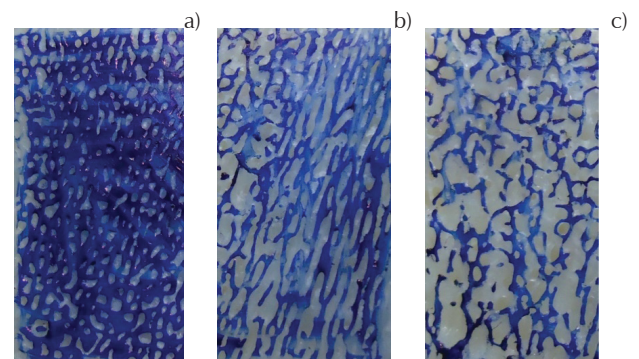


Figure 7. Trabecular bone images, where the different regions of the specimen are showed: a) region 1 b) region 2 and c) region 3

In the methodology of Saha and Wehril (2004) a method of scanning was used on the trabeculae to generate the respective ellipses, in this case, that scanning was omitted and instead two points were directly taken from the trabecular bone image.

One of the points is taken at the trabecula union zone. This point aim is to obtain major axis of the ellipse, based on the calculation of the distance between this point and the midpoint. The second point was taken at the edge of the corresponding trabecula, this point should be at an angle of 90 degrees to the trabecula major axis, which allowed calculating the ellipse minor axis.

The inclination angle of the ellipse was calculated generating a vector between the center point of the trabecula and the point obtained to calculate the major axis, the angle of this vector was obtained and this was considered as the inclination angle. Figure 9 shows the points and the inclination angle for one trabecula.

From the above points it may be generated a representation with ellipses of a whole trabecular structure, this representation was useful because the later construction of the model in Abaqus™ through Python™ programming language, needed an assignation of a number to each ellipse in order to build two lists.

The first list was named pores list, it is associated with the pores within the trabecular structure. This list contains other lists, which indicate the ellipses that are around every pore. That means the internal lists amount

equals the pores amount. The second list was named contour list, it is associated with ellipses that are on the periphery of the obtained structure, in order to get an outline to the final model. The amount of elements of the second list should be equal to ellipses amount that are on the periphery of the representation. Figure 10 shows the described previous steps, using an example of a trabecular structure represented by ellipses.

The models construction process was done to generate a programming code to take data from the points coordinates obtained from the trabecular bone image, the pores list and contour list. In order to obtain the corresponding points to each pores, first it was programmed command lines that calculated an intermediate point on each pore, and then a vector was generated from central point of each trabecula to central point of corresponding pore (pore vector). This was controlled by the pores list. Figure 11 shows a midpoint of a pore and the respective pore vectors to each corresponding trabecula.

Then, a function was defined to make a comparison between angle of pore vector and the inclination angle of each ellipse. If the inclination angle were greater than the pore vector angle, the angle value of pore vector would be subtracted to the inclination angle, if the subtraction were less than 180° a tangent point on the corresponding ellipse would be placed at an angle 90° less than the inclination angle of the ellipse, if it were greater, the tangent point would be placed at an angle

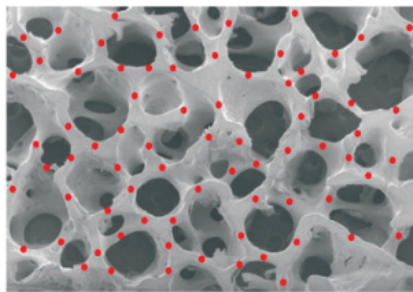


Figure 8. Midpoints assignation for some trabeculae in cancellous bone. Image at 200X (Narváez, 2004)

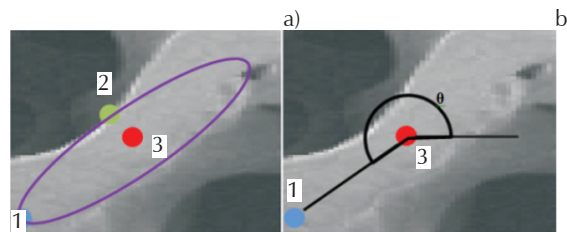


Figure 9. Process to represent trabeculae from ellipses: a) points assignation to calculate the major axis (1) and the minor axis (2), from the central point (3) and b) inclination angle of the ellipse

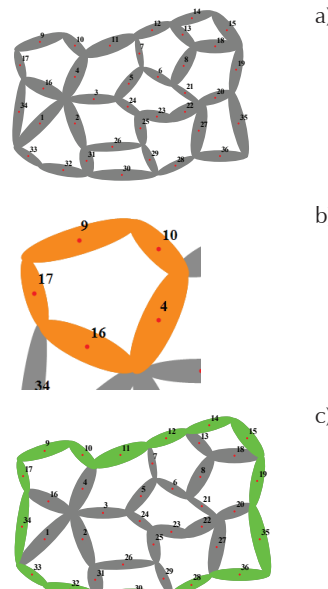


Figure 10. Previous analyses that were required to build the model: a) assigned numbers to each ellipse, b) ellipses that surround a pore and c) contour ellipses that help to form the outline of the model

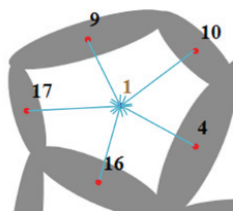


Figure 11. Pore vectors with their respective pore and trabeculae

90° higher. If the inclination angle were less than the pore vector angle, then the value of inclination angle would be subtracted to the angle value of pore vector, if the subtraction were less than 180° a tangent point on the corresponding ellipse would be placed at an angle 90° higher than the inclination angle of the ellipse, if it were greater, the tangent point would be placed at an angle 90° less.

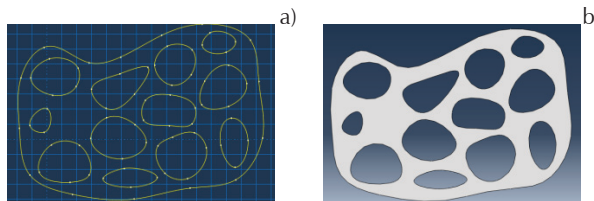
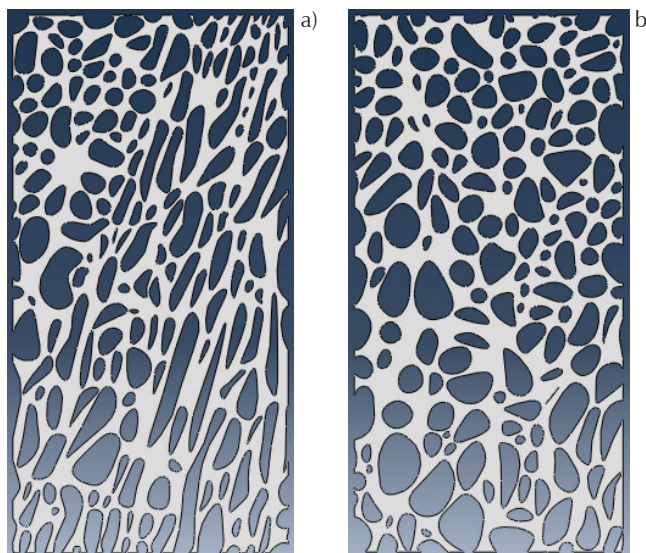


Figure 12. Two-dimensional model for an example of trabecular bone: a) sketch made by the spline tool and b) two-dimensional model built from the described methodology



For generating the curve which delimits the contour of the model using the spline tool, it had to be defined within the programming code some instructions to obtain tangent points to the ellipses.

Figure 12a shows the sketch made by spline tool that represents pores and outline of the used example. Figure 12b shows the two-dimensional model generated by Abaqus™.

After the models were generated, they were cut through Abaqus™ tools to contain each model in a rectangular area (2 cm x 1 cm).

That was done to represent the area of the intermediate parallel plane to the main axis of a cylindrical trabecular bone specimen (Figure 13).

The models that were generated using this methodology from the selected regions, are shown in Figure 14. In turn, Table 1 shows the most relevant data about each model.

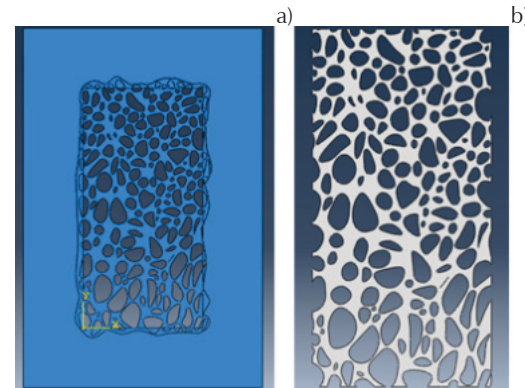


Figure 13. The cut of each model to delimit them in a rectangular area: a) frame in Abaqus® that made the cut and b) model that has been cut



Figure 14. Trabecular bone models generated by the described methodology for the different regions:  
a) region 1, b) region 2 and c) region 3

Table 1. Relevant data about generated models

Model	Amount of trabeculae	Amount of pores	Trabecular average thickness [mm]	Trabecular preferential orientation	Area fraction
Region 1	532	196	0.258±0.073	80°-105°	48.39%
Region 2	619	209	0.257±0.077	55°-80°	54.39%
Region 3	1120	375	0.251±0.058	75°-100°	65.6%

In order to test the models, a simulation of a mechanical compression test was conducted using Abaqus™, very simple conditions were assigned, because it was only intended to show that the methodology is useful for generating closer models to reality. First, a restricted movement condition was established on the base to each model, also a self-contact condition without friction was assigned to the trabeculae of each model and in each one was used a triangular elements mesh. Moreover, plane stress conditions were considered for each simulation. Then an analytical rigid part was placed on the top of each model, which moved 0.89 mm, this value corresponds to 5.5% deformation (Ramírez *et al.*, 2010). Among each model and the compression plate it was assigned a friction coefficient equals 0.27 (Davim and Marques, 2004).

In turn, the material properties were considered isotropic. A Young's modulus of 1.678 GPa was assigned, that was obtained using empirical formula of Rho (1993) from a bulk density equals 0.4 g/ cm<sup>3</sup> (Guerrero, 2014). Furthermore, it was established a Poisson's ratio equals 0.3 and it was assigned a density equals 1.8 g/cm<sup>3</sup> (Ruiz, 2010). Also, it was considered a maximum compressive strength equals 100 MPa (Cowin, 2001).

## RESULTS

This section shows the results about the compression tests. The first model used a mesh with 23,950 triangular elements.

Figure 15a shows the stress level in this model through a color scale, where the gray areas are those that have exceeded the maximum strength. In this analysis, it can be seen that only some trabeculae in this structure have exceeded the maximum strength, they are mainly in the section near the base, in the upper right corner area and some intermediate trabeculae. That means the load distribution along the structure focuses on these described sections.

The second model used a mesh with 30,692 triangular elements. Figure 15b shows the stress level through the structure. Areas that have overcome the strength value include some diagonal trabeculae localized from

the lower left corner to the upper right corner of the model, then, the trabeculae that have failed are those that have a preferential orientation and load is transmitted through this zone.

For third model that corresponds to region 3, the used mesh contained 40,245 triangular elements. Figure 15c shows the stress level through structure. If it is compared with previous models, this model has a greater number of zones with a different color to blue, that means, the most elements in this structure are working to distribute the load, so then it is performed a uniform stress distribution.

Figure 16a shows a comparison about the reaction force versus displacement curves of three models.

This graph shows the apparent slope changes in model 2 compared to the other two models, this happened because interactions occurred among the trabeculae.

It can be appreciated that third model presents the strongest reaction force of three models, this is because it is the model that has the largest area fraction and also it has an adequate architecture for the established load.

Furthermore, figure 16b shows a graph about maximum reaction force versus area fraction for the three models, in this graph it can be seen, how the area occupied by a model causes variations in the reaction force.

It is important to say that the area fraction can be considered equal to the volume fraction (Ruiz, 2013). However, it should be noted that the reaction force does not increase linearly with the area fraction, this is due to the architecture of each model.

When comparing these three models using percentages, it can be seen that the model 2 has a 12.6% higher area fraction than model 1, and in turn it has a 23.8% higher reaction force than model 1. Model 3 has a 20.61% higher area fraction and a 73.54% higher reaction force than model 2. Furthermore, model 3 has a 35.81% higher area fraction and a 114.86% higher reaction force than model 1.

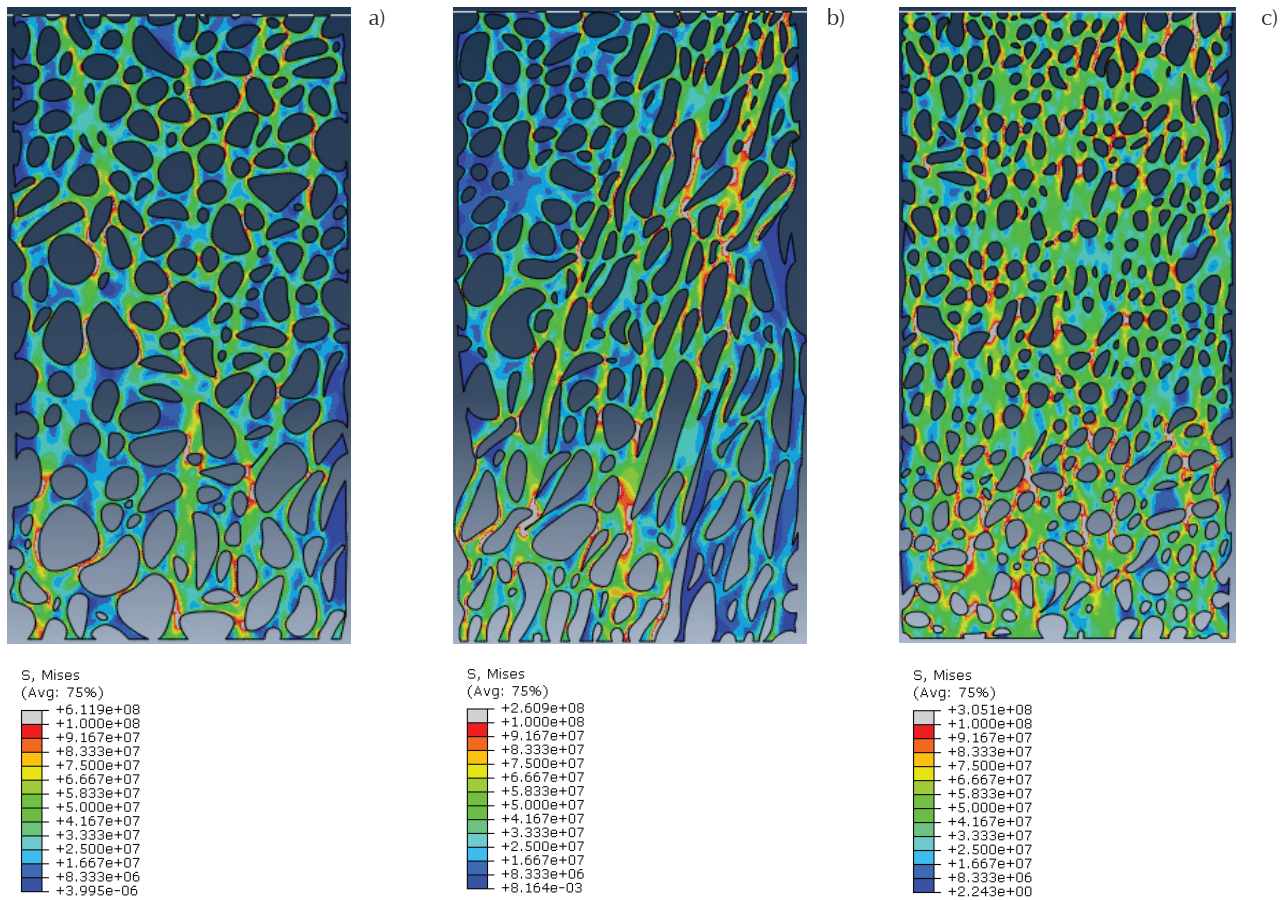


Figure 15. Von Mises stress level for three generated models at 5.5% strain: a) region 1, b) region 2 and c) region 3

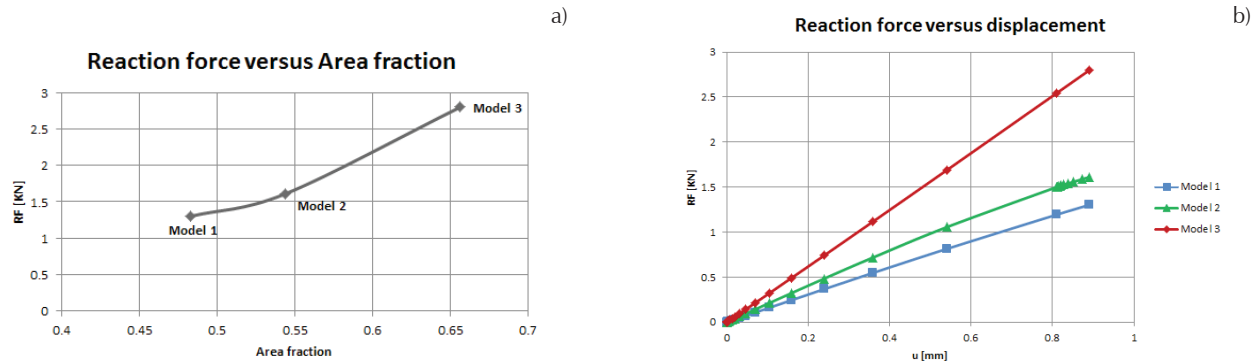


Figure 16. a) Reaction force versus displacement of each model and b) maximum reaction force versus area fraction of each model

## CONCLUSIONS

For proposed methodology, in terms of models that can be obtained, the final geometries and structures that can be represented are very similar to the geometries and structures that appear in the original images. This is corroborated by three obtained models in this work, because each one represents a different trabecular bone image.

At the simulations, it was possible to see that the different architectures and different area fractions, affect the final results, both the failure regions and the behavior of the graphs about reaction force versus displacement and maximum reaction force. Furthermore, the shown percentages confirm the area fraction effect in the structure stiffness, where model 3 had considerable percentage increases, because it had 20.61% more area fraction than model 2, this increased its reaction force 73.54% more, however this is most clearly seen when comparing model 3 and model 1, where model 3 had 35.81% more area than model 1, this caused that reaction force increased by 114.86%, that is, it was more than double what model 1 could give.

Because in each simulation the same characteristic test parameters and the same mechanical properties were established, the difference among results depends only on the structure formed by the trabeculae and area fraction occupied by bone.

## ACKNOWLEDGEMENTS

This work was supported by Dirección General de Asuntos del Personal Académico, UNAM, under grants IN115415. The authors would like to thank Álvarez G., Cueva I., Ramos E. and Morales L. for technical assistance during the elaboration of this study.

## REFERENCES

Bevill G. and Keaveny T.M. Trabecular bone strength predictions using finite element analysis of micro-scale images at limited spatial resolution. *Bone*, volume 44 (issue 4), 2009: 579-584. Doi:10.1016/j.bone.2008.11.020. Bone 44. USA.

Depalle B., Chapurlat R., Walter-Le-Berre H., Bou-Said B., Follet H. Finite element dependence of stress evaluation for human trabecular bone. *J. Mech. Behav. Biomed. Mater.*, volume 18, 2012: 200-212.

Kowalczyk P. Elastic properties of cancellous bone derived from finite element models of parameterized microstructure cells. *Journal of Biomechanics*, volume 36, 2003: 961-972.

Ramírez-Díaz E.I., Ortiz-Prado A., Schouwenaars-Franssens R., Ruiz-Cervantes O. Metodología para el modelado del comportamiento mecánico de hueso esponjoso a partir de sus microestructuras. *Ingeniería, Investigación y Tecnología*, volume 11 (issue 2), 2010: 199-216. Recuperado: 07 de marzo de 2016, de [http://www.scielo.org.mx/scielo.php?script=sci\\_arttext&pid=S1405-77432010000200007&lng=es&tlng=es](http://www.scielo.org.mx/scielo.php?script=sci_arttext&pid=S1405-77432010000200007&lng=es&tlng=es).

Saha P.K. and Wehrli F.W. A robust method for measuring trabecular bone orientation anisotropy at in vivo resolution using tensor scale. *Pattern Recognit*, volume 37, 2004: 1935-1944.

Narváez M. *Métodos para el análisis de la microestructura y propiedades mecánicas del hueso esponjoso* (thesis), Facultad de Ingeniería, Universidad Nacional Autónoma de México, 2004.

Davim J.P. and Marques N. Dynamical experimental study of friction and wear behaviour of bovine cancellous bone sliding against a metallic counterpart in a water lubricated environment. *Journal of Materials Processing Technology*, volume 152 (issue 3), October, 30 2004: 389-394. ISSN 0924-0136, <http://dx.doi.org/10.1016/j.jmatprotec.2004.04.420>.

Rho J.Y., Ashman R.B., Turner C.H. Young's modulus of trabecular and cortical bone material: Ultrasonic and microtensile measurements. *J Biomech*, volume 26, 1993:111-119.

Guerrero L. *Análisis de un modelo de hueso femoral mediante FEM* (thesis) Facultad de Ingeniería, Universidad Nacional Autónoma de México, 2014.

Ruiz O. *Efecto en la resistencia mecánica del hueso esponjoso al variar la densidad y la arquitectura trabecular* (master thesis), Facultad de Ingeniería, Universidad Nacional Autónoma de México, 2010.

Cowin S. *Bone Mechanics Handbook*, USA, FL:CRC Press, 2001.

Ruiz O.R. *Caracterización de hueso esponjoso bovino mediante la medición de parámetros microestructurales* (thesis), Facultad de Ingeniería, Universidad Nacional Autónoma de México, 2013.

## BIBLIOGRAPHY

Ángeles J. *Caracterización mecánica del comportamiento viscoelástico de muestras de hueso trabecular bovino* (thesis), Facultad de Ingeniería, Universidad Nacional Autónoma de México, 2014.

Morgan E., Bayraktar H., Keaveny T. Trabecular bone modulus-density relationships depend on anatomic site. *Journal of biomechanics*, volume 36, 2003.

Cerrud S., Narváez M., Muñoz V., Schouwenaars R. Modelado del comportamiento mecánico del hueso (análisis de los efectos del grado de hidratación). *Mexican Society of Mechanical Engineering*, volume 1, Mexico, 2005.

**Suggested citation:**

**Chicago style citation**

Ruiz-Cervantes, Osvaldo, José Salvador Lara-Ramírez, Edgar Isaac Ramírez-Díaz, Armando Ortiz-Prado. Trabecular bone modeling methodology using geometric representations. *Ingeniería Investigación y Tecnología*, XVIII, 04 (2017): 379-387.

**ISO 690 citation style**

Ruiz-Cervantes O, Lara-Ramírez J.S., Ramírez-Díaz E.I., Ortiz-Prado A. Trabecular bone modeling methodology using geometric representations. *Ingeniería Investigación y Tecnología*, volumen XVIII (issue 4), October-December 2017: 379-387.

**ABOUT THE AUTHORS**

*Osvaldo Ruiz-Cervantes.* He obtained his Master degree in Materials Science and Engineering from UNAM IIM, and currently developing a PhD in Mechanical Engineering at UNAM. Has worked on different topics like manufacture processes simulation and trabecular bone structure analysis using ABAQUS™.

*José Salvador Lara-Ramírez.* He received the bachelor degree in Mechanical Engineering from Engineering Faculty of the National Autonomous University of Mexico (UNAM) in 2015. He worked in the Centre for Research and Technical Assistance on Materials (UDIATEM) of UNAM from 2013 to 2015, where he did his social service researching new methodologies whose objective was to analyze virtual models of cancellous bone through finite element method. His professional interests are focused in mechanical design, material engineering and manufacturing processes.

*Edgar Isaac Ramírez-Díaz.* He obtained his Master degree in Materials Science and Engineering from UNAM IIM, and currently developing a PhD in mechanical engineering at UNAM. Has worked on different topics like manufacture processes and bone tissue models using ABAQUS™

*Armando Ortiz-Prado.* Mechanical and Electrical Engineering from engineering school of UNAM (1980), where he also earned a Masters and Doctorate in Mechanics. He has taught Continuum Mechanics, Manufacturing Process Modeling and Science Materials. His research interests include modeling Mechanical Forming Processes, Failure analysis, Mechanical Behavior of Biomaterials and Corrosion in electronic equipment. His productivity also includes 18 articles in international conferences, over 80 articles in national conferences and more than 20 articles in journals.